Desalination and Water Treatment
www.deswater.com

doi: 10.5004/dwt.2017.21447

96 (2017) 112–119
November

Preparation and characterization of mesoporous silica (Ms) supporting lanthanum carbonate (Ms-La) for the defluorination of aqueous solutions

Rui Wang[a,†], Lijun Luo[a,†], Yong JunYang[a], Li Shu[b], Veeriah Jegatheesan[b], Hongbin Wang[a,*], Min Yang[a,*]

[a]*School of Chemistry and Environment, Yunnan Minzu University, Kunming 650500, China, emails: 595530820@qq.com (H.B. Wang), 826677468@qq.com (M. Yang), 392639402@qq.com (R. Wang), 10501931@qq.com (L. Luo), 1060656032@qq.com (Y.J. Yang)*
[b]*School of Engineering, RMIT University, Melbourne, Victoria 3000, Australia, emails: li.shu@rmit.edu.au (L. Shu), jega.jegatheesan@rmit.edu.au (V. Jegatheesan)*

Received 24 June 2017; Accepted 9 September 2017

ABSTRACT

In this paper, the mesoporous silica (denoted as Ms) was modified by lanthanum and the optimal preparation conditions were investigated for lanthanum loaded mesoporous silica materials (denoted as Ms-La). The Ms-La material was characterized by scanning electron microscopy (SEM), X-ray diffraction (XRD), Fourier transform infrared spectroscopy (FTIR) and Thermogravimetric analysis-differential temperature analysis (TG-DTA). The results show that lanthanum is successfully loaded onto the surface of the Ms, and the structure of the Ms did not change during the loading process. The Ms-La had good defluorination performance due to its large surface area and good dispersive effect. The defluorination by the Ms-La can reach 81% before optimization and can reach 90% under optimum conditions (nNaHCO$_3$/nLa = 3.0, nLa/nSi = 0.08 and 90°C drying temperature). The results of isotherm experiments showed that the maximum adsorption capacity was 19.85 mg/g, and the adsorption was in accordance with Langmuir isotherm adsorption model and the adsorption process was mainly based on the replacement of CO_3^{2-} from $La_2(CO_3)_3$ by F^- to form $La(CO_3)F$.

Keywords: Mesoporous silica; Lanthanum carbonate; Fluoride removal

1. Introduction

Fluorine is one of the trace elements in the human body and other biological species. But excessive intake of fluorine will bring harm to human body by the inhibition of biological activity and to plants by the inhibition of photosynthesis [1]. The World Health Organization regulates fluoride content in drinking water which must not exceed 1.5 mg/L. The fluoride content in drinking water in China shall not exceed 1.0 mg/L. Therefore, how to effectively reduce the fluorine content present in the industrial wastewater is an important livelihood issue [2]. At present, there are many methods to remove fluoride from industrial wastewater, such as adsorption, chemical precipitation, ion exchange, membrane separation, electrical agglomeration, etc. [3–5]. Adsorption is the most effective method for the removal of fluoride because of the following advantages: (i) little secondary pollution, (ii) high removal efficiency and (iii) safe and simple operating procedures [6]. The adsorbents commonly used in water treatment process include activated carbon, ion exchange resin and silica gel. But single adsorbent cannot completely remove a particular pollutant present in the

* Corresponding author.

† Authors contributed equally to this work.

Presented at the 9th International Conference on Challenges in Environmental Science & Engineering (CESE-2016), 6–10 November 2016, Kaohsiung, Taiwan, 2016

water because of the existence of other pollutants in various formations. So it is necessary to explore complex adsorbents [7]. Mesoporous materials are the materials with pores with 2–100 nm in size, which possess excellent characteristics such as regular pore channel and larger surface area and widely used in biological materials, photochemistry, electrochemistry, adsorption, catalysis, etc. [8,9]. Mesoporous silica is one of the most popular and effective mesoporous materials, which has high specific surface area, adjustable channel and can be modified easily. Mesoporous materials, especially those with ordered pore systems, endow huge interface to accommodate guest species as well as have feasibility for functionalization; which are necessary requirements for excellent adsorbents [10].

Rare earth metals are distributed in the earth's crust, and China has the most rare earth reserves in the world [11]. Rare earth hydrated ferric oxide and rare earth salts have strong affinity to inorganic ions in aqueous solution such as fluorine, arsenate, phosphate and other inorganic anions. Therefore, they can effectively remove inorganic ions in water, such as fluoride, phosphorus, arsenic, ammonia nitrogen, chromium, cadmium and other pollutants by adsorption [12,13]. In this work, we intend to modify mesoporous silica (Ms) by the rare earth metal lanthanum to obtain lanthanum loaded mesoporous silica (Ms-La) and remove fluorine ion from water by adsorption.

2. Materials and methods

2.1. Preparation of Ms

Ms was synthesized using the method reported by Li et al. [14] where 21 mL of hexadecyltrimethylammonium bromide (CTAB) was dissolved in 100 mL of distilled water. Then 50 mL of ethanol was added to the solution and stirred with a magnetic stirrer until CTAB was dissolved fully. 12 mL of concentrated aqueous ammonia was added dropwise into the mixture. After stirring for 15 min, 3.5 mL of tetraethyl orthosilicate was added dropwise and a white precipitate appeared gradually. The white precipitate was kept stirred and allowed to settle for 2 h. Then the precipitate was filtered, washed and dried at 70°C in vacuum overnight, and finally calcined at 550°C for 3 h to synthesize Ms (surface area = 1,363 m^2/g, total pore volume = 0.876 cm^3/g and average pore size = 3.30 nm).

2.2. Preparation of Ms-La composite

In the preparation process, sol-gel method was used to prepare rare earth metal doped Ms. A certain amount of prepared Ms was dispersed in deionized water, and then a corresponding amount of lanthanum carbonate according to La/Si molar ratio was added into it. The lanthanum carbonate was dissolved thoroughly in this dispersed solution. While stirring, $NaHCO_3$ was added slowly to the above mixed solution as a precipitant. After further 10 h of stirring, the Ms-La composite was obtained. The Ms-La composite was washed and harvested with centrifugation/re-dispersion cycles and dried at 550°C for 3 h.

In order to study the effect of the $NaHCO_3$/La molar ratio on the adsorption performance, 0.3 g of Ms-La dispersed in 30 mL of deionized water; 0.1 molar ratio of La/Si rare earth metal salts was added into the above solution and dissolved in the mixed dispersion solution after stirring; 30 mL of different molar ratios of $NaHCO_3$/La (1.5, 2.0, 3.0, 4.0, 5.0 and 6.0) solution were added dropwise into the above solution and stirred continuously for 10 h. Then filtered, washed and dried at 90°C in vacuum.

In order to investigate the molar ratio of La/Si on the adsorption performance, 30 mL of different mole ratio of La/Si (0.02, 0.04, 0.06, 0.08, 0.10, 0.08 and 0.10) solutions were used to prepare Ms-La composites under optimum preparation conditions.

In order to investigate the effects of calcination temperature on the adsorption performance, Ms-La composites prepared under optimum conditions were calcinated (at 90°C, 200°C, 300°C, 400°C, 500°C, 600°C and 500°C) to obtain the temperature effects on the removal of fluoride.

2.3. Adsorption experiment

The defluorination properties of the Ms-La composite were performed by monitoring changes of F^- concentration in the solution. The typical procedure used was as follows: 0.10 g of Ms-La was added into a conical flask. 50 mL of solution containing 10 mg/L of F^- was transferred into this flask. Then the flask was shaken at 200 rpm for 3 h at 25°C. After that, the solution was centrifuged, and the concentration of F^- in the supernatant was determined by GB7484-1987 analysis method (water and water quality monitoring analysis method) [15]. These were then repeated three more times. The removal percentage was used to evaluate the performance of rare earth modified Ms materials. Adsorption removal percentage can be expressed as $(C_0 - C_t)/C_0 \times 100\%$, where C_0 (mg/L) and C_t (mg/L) are the initial and time t concentrations of the fluorine, respectively. The adsorption capacity can be expressed as $(C_0 - C_t) \times V/(m \times 1{,}000)$ where V is the volume of the solution and m is the mass of the adsorbent, Ms-La composite.

2.4. Characterization

The morphology of Ms-La was observed on a field emission scanning electron microscope (FEI-Nova, NanoSEM450, USA). The crystallographic structures were characterized by XRD (Rigaku, Japan) with Cu-Ka radiation (45 kV, 250 mA) and a continuous scan mode was employed with a scan rate of 10 min^{-1} with 2θ ranging from 10° to 80°. FT-IR spectrum was obtained by a spectrometer (NICOLETIS10) with powder samples embedded in KBr disks. The prepared materials were analyzed by the thermogravimetric analysis-differential temperature analysis (TG-DTA, STAA49F31, Germany).

3. Results and discussion

3.1. Adsorption

F removal with three adsorbents namely Ms (SiO_2 carrier), Ms-La (SiO_2-La) and pure $La_2(CO_3)_3$ was measured. The results showed (Fig. 1) that the F^- removal by Ms was only 6.4% and by pure $La_2(CO_3)_3$ was 59.5%. But the F^- removal rate of Ms-La was up to 81%. The results indicate that the removal of F^- by Ms-La has been enhanced significantly. The main reason may be that the dispersion of the active ingredients increased after loading, which was beneficial in making contact with fluorine ions [16,17].

3.2. Characterization of Ms-La

3.2.1. SEM analysis

Adsorbents such as Ms-La under different molar ratios of La/Si (La/Si = 0.02, 0.08 and 0.20), pure $La_2(CO_3)_3$, pure SiO_2 and La/Si = 0.08 after adsorption were observed under SEM in order to compare the morphologies (Fig. 2). According to Fig. 2, pure $La_2(CO_3)_3$ material was similar to sheets arranged to form flakes (Fig. 2(d)). The SEM images (Fig. 2(f)) show the spherical shaped growth of SiO_2 clearly. Compared with the pure $La_2(CO_3)_3$ and pure SiO_2, lanthanum had been successfully loaded on the Ms surface in Ms-La. There was a small amount of carbonate precipitation found on the surface of Ms when the molar ratio of La/Si was 0.02. Sheet material also increased on the surface of Ms, and the degree of accumulation and deposition became higher with the increase in the molar ratio of La/Si. The reason was that lanthanum carbonate could not be completely co-precipitated on the surface of Ms or into the channels. Because of the degree of accumulation was too high, F^- was unable to fully contact with the adsorbent, and therefore the utilization rate of adsorbent was low. This was reflected in the level of adsorption, which was not improved significantly after increasing the lanthanum content beyond a certain value [18]. According to Fig. 2(e), it can be seen that there was a small amount of lanthanum carbonate on the surface of Ms-La at the La/Si = 0.08 before the adsorption Fig. 2(b). Compared with that Fig. 2(b), the shape of Ms-La after adsorption changed and obviously the small amount of sheet deposits that were present originally disappeared, and small white particles were formed (Fig. 2(e)). This indicates that the adsorbents and the adsorbate had reacted fully.

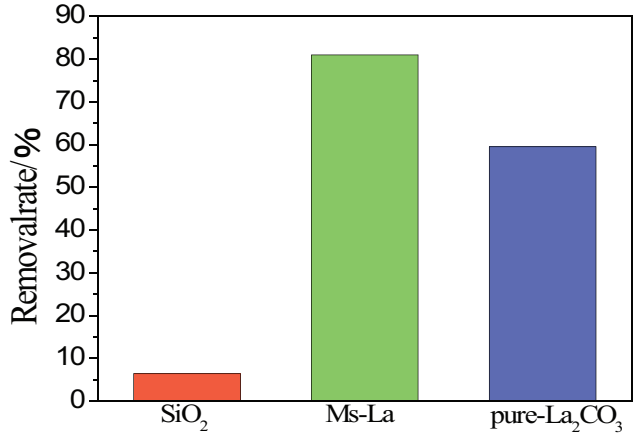

Fig. 1. Effect of different absorbents on F^- removal.

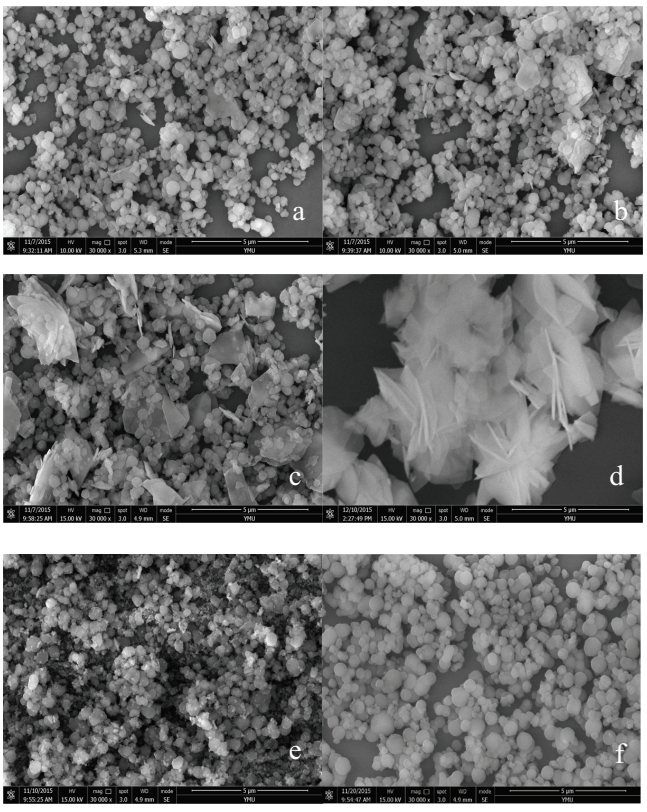

Fig. 2. SEM images of different La/Si molar ratio (a) La/Si = 0.02; (b) La/Si = 0.08; (c) La/Si = 0.20; (d) pure $La_2(CO_3)_3$; (e) La/Si = 0.08 (after adsorption) and (f) pure SiO_2.

3.2.2. XRD analysis

In order to investigate the crystal phase structure of prepared materials, the XRD spectra of Ms (SiO_2 carrier), pure $La_2(CO_3)_3$ and Ms-La (SiO_2-La) were obtained as shown in Fig. 3(a). It can be seen from Fig. 3(a) that the new diffraction peak coincided with the standard card JCPDS 29-0085, which illustrates that the new diffraction peak is SiO_2. The Ms-La still retained the original $La_2(CO_3)_3$ characteristics of diffraction peak; the peak position had no bias shift, and the mesoporous structure had not been damaged. Since the content of $La_2(CO_3)_3$ was low, the peak intensity diminished compared with pure Ms. The reason may be that some channels of Ms could have been blocked, and crystallinity was also weakened, but the mesoporous structure had not been damaged.

In order to further investigate the effect of calcination temperatures on the crystal phase structure, the XRD spectra of Ms-La at different calcination temperatures were obtained as shown in Fig. 3(b). The diffraction peak of lanthanum carbonate was gradually weakened with the increase in calcination temperature. There appeared new diffraction peaks when the calcination temperature was above 500°C, which coincided with the standard card JCDP48-1113. This illustrated that carbonate had been decomposed into $La_2O_2CO_3$ at 500°C. Some characteristic peaks coincided with the standard card JCDP54-0213 at 700°C. This indicates that the material has began to decompose into La_2O_3 at 700°C.

The XRD spectra of Ms-La before and after adsorption are shown in Fig. 3(c). When comparing the two curves (before and after adsorption), we can see that the diffraction peak obviously changed after adsorption, indicating that the nature of the adsorbent has changed significantly after the adsorption. The new diffraction peak coincided with the standard card JCDP41-0595, which illustrates that $La(CO_3)F$ has been formed after the adsorption. The adsorption process may be that the CO_3^{2-} of $La_2(CO_3)_3$ was partially replaced by the F^- [19], At the same time there was a new diffraction peak which illustrates the formation of a small amount of LaF_3 [20].

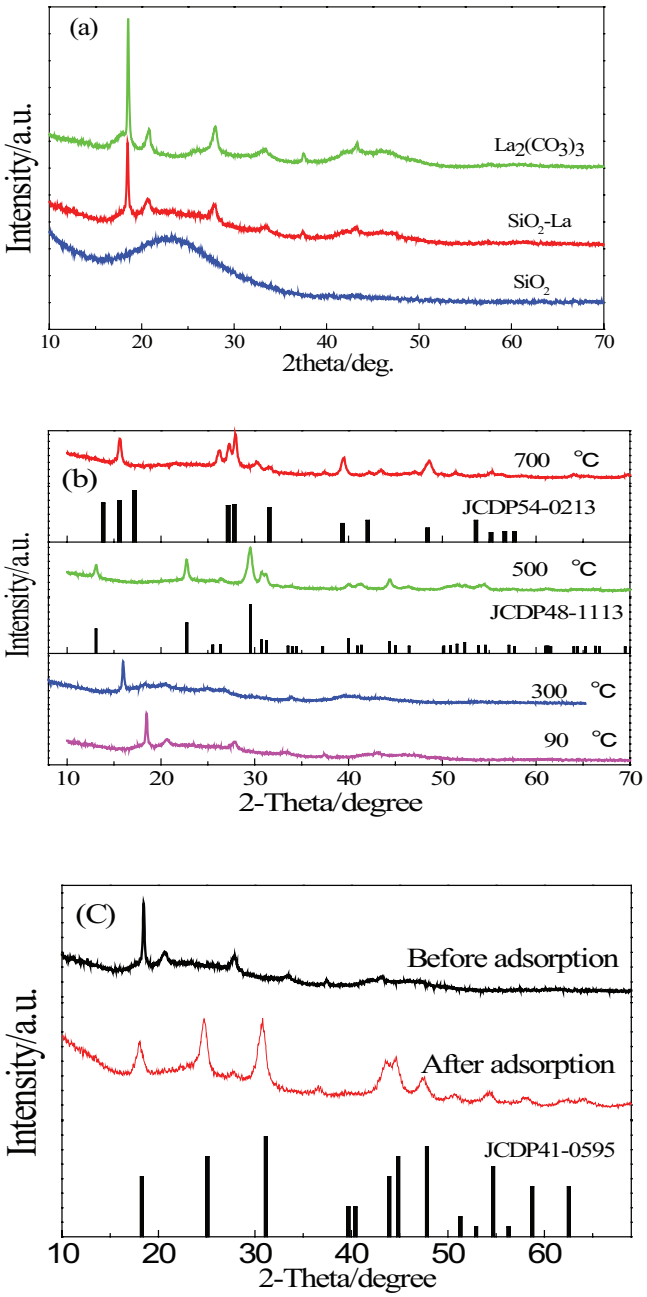

Fig. 3. XRD spectra of (a) Ms (SiO_2 carrier), pure $La_2(CO_3)_3$ and Ms-La (SiO_2-La). (b) XRD spectra of Ms-La at different calcination temperatures. (c) XRD spectra of the adsorbent before and after adsorption.

3.2.3. FTIR analysis

The FTIR spectra of Ms-La at different calcination temperature are shown in Fig. 4. It can be seen that absorption peaks were mainly the characteristic peaks of Ms at 806, 1,089, 1,637 and 3,450 cm^{-1} (Fig. 4(a)). From Fig. 4(b), it can be seen that Ms-La before the adsorption still retained the characteristic peaks of lanthanum carbonate and silicon dioxide. The strong absorption peak at 3,450 cm^{-1} was generated by OH^- of the sample anti-symmetric stretching vibration in the crystal water and adsorbed water. Two strong absorption peaks at

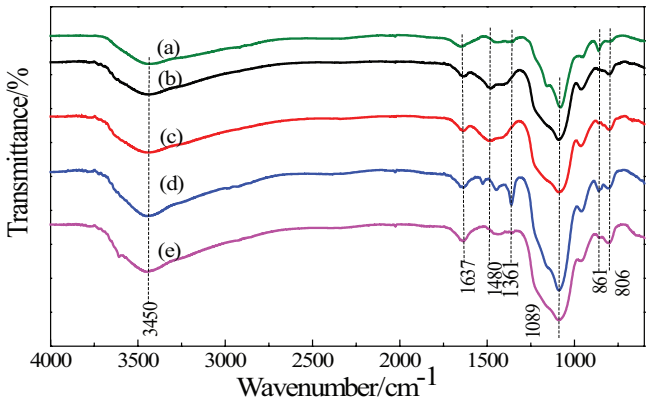

Fig. 4. Infrared spectra of the adsorbent with different calcination temperature (a) 25°C of SiO_2; (b) 90°C; (c) 300°C; (d) 500°C and (e) 700°C.

1,300–1,600 cm^{-1} were stretching vibration of CO_3^{2-} group of carbonate salt. Small absorption peaks at 861 cm^{-1} were bending vibrations of CO_3^{2-} group of carbonate salt. Absorption peak at 1,089 cm^{-1} was the frequency of the non-degenerate vibration absorption of carbonate. With the increase of temperature, the calcined material still retained the characteristic peak of mesoporous silica, and the two strong absorption peaks of CO_3^{2-} group at 1,361 and 1,480 cm^{-1} were shifted to change a wide peak [21]. The main reason was that $La_2(CO_3)_3$ was generated into $La_2O_2CO_3$ at high temperature. At temperatures above 500°C, the absorption peaks at 1,089 cm^{-1} are enhanced. The reason was that the characteristic peaks of the carbonate gradually disappeared as the temperature continued to increase. $La_2(CO_3)_3$ was generated into La_2O_3 at high temperature.

3.2.4. TG-DTA analysis

According to Fig. 5(a), the decomposition process of carbonate lanthanum by heating can be divided into three stages: first, the surface adsorbed water and crystal water were removed at 50°C–350°C, and the weight loss rate was 4.84%, which was consistent with the theoretical value (the proportion of water molecules in $La_2(CO_3)_3 \cdot H_2O$ was 3.78%). Second, the weight loss rate was 18.41% at 350°C–600°C, and the two CO_2 molecules might have been removed, which was consistent with the theoretical basis of 18.48%. Third, the weight loss rate was 8.70% at 600°C–850°C and the sample lost a CO_2 molecule that was consistent with the theoretical basis of 9.24%. Therefore, the transformation of $La_2(CO_3)_3 \cdot H_2O$ due to heating process was as follows:

$$La_2(CO_3)_3 \cdot H_2O \rightarrow La_2(CO_3)_3 \rightarrow La_2O_2CO_3 \rightarrow La_2O_3 \quad (1)$$

It can be seen from Fig. 5(b) that the proportion of lanthanum carbonate was 23.4% in Ms-La. The first weight loss stage was that adsorbed water and lanthanum carbonate crystal water, and the weight loss ratio was 10.55%. In the second stage, Ms-La lost two CO_2 molecules, and the 5.24% weight loss was consistent with the theoretical value of 4.32%. In the third stage, the samples of lanthanum carbonate lost a CO_2 molecule, the 2.81% weight loss rate was consistent with the

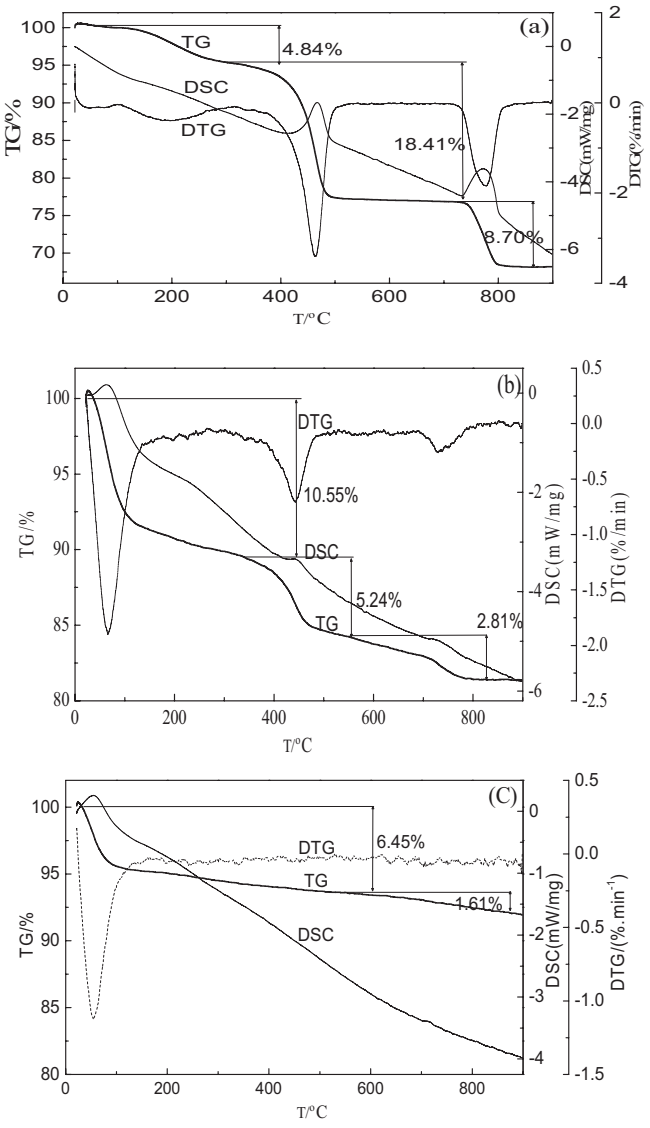

Fig. 5. TG-DTA patterns of (a) pure $La_2(CO_3)_3$, (b) Ms-La and (c) Ms.

theoretical value of 2.16%. From Fig. 5(c) it can be seen that Ms still has a small weight loss ratio after 550°C because a small amount of template decomposing agent remained in Ms.

3.3. Optimization of synthesizing conditions of Ms-La

3.3.1. The effect of precipitating agent on adsorption performance

In order to investigate the effect of precipitation agents on the adsorption performance, Ms was modified by $NaHCO_3$, NH_4HCO_3, $NH_3{\cdot}H_2O$ and Na_2CO_3. The effect of fluorine removal was shown in Fig. 6(a). From Fig. 6(a), we can see that the materials prepared by different precipitation agents had great effect on the removal rate of fluoride ions. The removal rate can reach 40%, 80%, 90% and 90% by using $NH_3.H_2O$, NH_4HCO_3, $NaHCO_3$ and Na_2CO_3 as precipitant, respectively. The main reason may be that the preparation was not easy to control when Na_2CO_3 was used as a precipitation agent. It may produce alkali carbonate, and the removal rate of NH_4HCO_3 as precipitant was relatively low. So finally $NaHCO_3$ was chosen as the precipitant.

3.3.2. Effect of molar ratio of $NaHCO_3$/La on the adsorption of F^-

The effect of molar ratio of $NaHCO_3$/La (1.5, 2.0, 3.0, 4.0, 5.0 and 6.0) on fluoride removal was studied and the results are shown in Fig. 6(b). From Fig. 6(b), we can see that the molar ratio of $NaHCO_3$/La had less effect on removal percentage of fluorine. The main reason may be that rare earth element La can be entirely precipitated when the molar ratio was more than 3.0. However, when the molar ratio was less than 3.0, it cannot precipitate completely and therefore although the molar ratio of La/Si was smaller than the theoretical value of 0.1, it still had a good ability to remove fluorine. Finally, in order to ensure that precipitation reaction was complete and the synthesized materials had good adsorption performance, the mole ratio of $NaHCO_3$/La was selected as 3.0.

3.3.3. Effect of mole ratio of La/Si on the adsorption of F^-

The effect of different molar ratio of La/Si on the fluoride removal is shown in Fig. 6(c). It can be seen that the adsorption began to increase rapidly when the molar ratio increased from 0.02 to 0.06, and then it tended to be stable when the mole ratio of La/Si was 0.08. It was mainly due to the optimum deposition of La on Ms when the La content increased up to a certain amount. If the La content increased further, it led to its excessive overlay and existed alone. From the point of view on cost, the optimum mole ratio of La/Si was selected as 0.08 in this study.

3.3.4. Effect of calcination temperature on the adsorption of F^-

The effect of calcination temperature on the F^- removal is shown in Fig. 6(d). It can be seen from Fig. 6(d) that the effect was obviously with the increase of calcination temperature. The highest removal can reach about 90% under dried conditions at the temperature of 90°C without calcination. While calcination temperature was increased to 300°C, the removal reduced to about 40%. This illustrates that the calcination has a great influence on adsorption performance. The following can be attributed to this observation: first, the carbonate salts were decomposed into Ms and crystal structure was destroyed at high temperature, so the capacity of ion exchange of Ms-La became deteriorated. Second, due to the loss of exchanged hydroxyl after material dehydration and the reduction in the number of adsorption active sites, adsorption declined. In this study, the temperature was selected as 90°C.

Based on the above data analysis and discussion, the optimal conditions for synthesizing Ms-La when $NaHCO_3$ is selected as precipitant are: $n$$NaHCO_3$/$n$La = 3.0, nLa/nSi = 0.08 and the drying temperature = 90°C in vacuum. The typical preparation process is as follows: 0.375 g of Ms was dispersed in 30 mL of deionized water. A certain amount of lanthanum nitrate was added into the solution, and stirred until it is fully dissolved. Then 20 mL of $NaHCO_3$ solution was added dropwise into the above solution, and stirred continuously (at a

speed of 200 rpm) for 10 h. Then the adsorbent was filtered, washed and dried at 90°C in vacuum overnight.

3.4. Adsorption experiments

3.4.1. Adsorption isotherm

Langmuir model and Freundlich model are two commonly used models in most of the adsorption isotherm studies to describe the adsorption thermodynamics of a liquid–solid system. The Langmuir adsorption isotherm is as follows:

$$\frac{C_e}{Q_e} = \frac{1}{K_L Q_m} + \frac{C_e}{Q_m} \tag{2}$$

The Freundlich adsorption isotherm is as follows:

$$Q_e = K_f C_e^{1/n} \tag{3}$$

where Q_m (mg/g) is the adsorption capacity at saturation; Q_e (mg/g) is the adsorption capacity at equilibrium; K_L and K_f are adsorption equilibrium constants, C_e is the adsorption mass concentration at adsorption equilibrium (mg/L) and n is an indication of how intense the absorption phenomenon is.

Under the optimum conditions, the effect of Ms-La material on the fluorine adsorption at different temperatures is shown in Fig. 7. At different temperatures, the fluoride

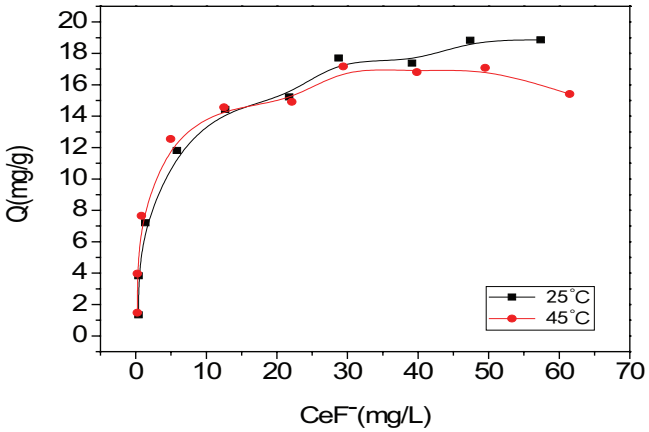

Fig. 7. Adsorption isotherms of fluoride ions at different temperatures.

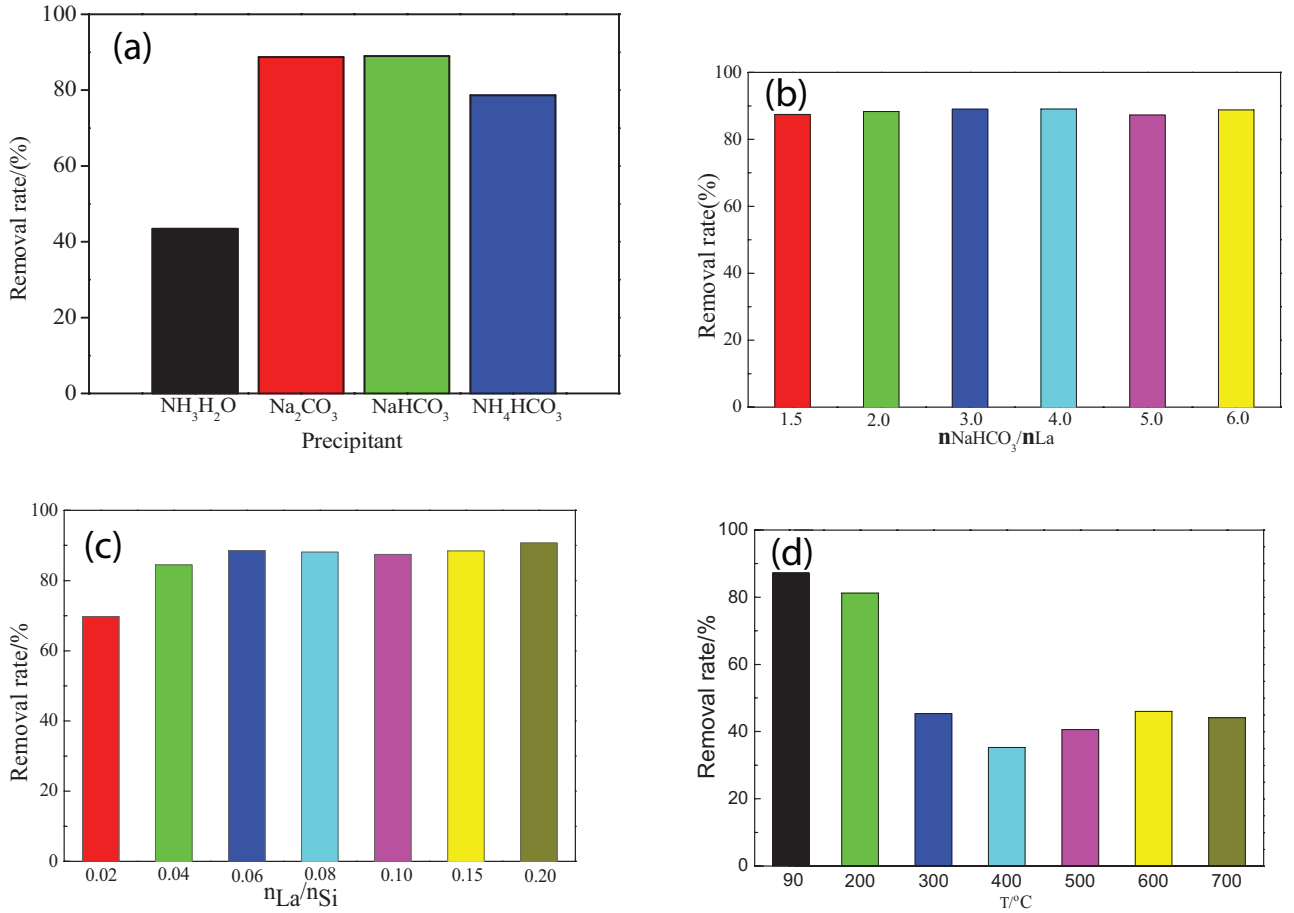

Fig. 6. (a) Effect of different precipitation agents on the removal of fluoride. (b) Effect of mole ratio of $NaHCO_3$/La on the removal of fluoride. (c) Effect of different mole ratio of La/Si on the removal of fluoride. (d) Effect of different calcination temperature on the removal rate for fluoride.

Table 1
Isotherm models and related fitting parameters

T (K)	Langmuir isotherm				Freundlich isotherm			
	Equation	Q_m (mg/g)	K_L (L/mg)	R^2	Equation	$1/n$	K_f	R^2
298	$Q_e = \frac{5.0406C_e}{1+0.254C_e}$	19.85	0.254	0.9968	$Q_e = 4.235C_e^{0.4162}$	0.4162	4.235	0.9158
318	$Q_e = \frac{13.9797C_e}{1+0.842C_e}$	16.60	0.842	0.9962	$Q_e = 5.190C_e^{0.3371}$	0.3371	5.190	0.8909

Note: R was the linear fitting correlation coefficient.

Table 2
Comparative assessment of literature on other fluoride adsorbents

Adsorbent	Adsorption capacity (mg/g)	Reference
Granular ferric hydroxide	7.0	[22]
Fe-Al-Ce nano-absorbent	2.22	[23]
Aluminium titanate	0.85	[24]
Bismuth aluminate	1.55	[24]
La-Ch	4.008	[25]
Chitosan–praseodymium complex	15.87	[26]
Palm stones	3.95	[27]
Ms-La	19.85	This work

adsorption capacity of the adsorbent increased with the initial concentration of fluoride in the solution. When the initial concentration was higher than 50 mg/L, the amount of adsorption tended to be the maximum, and at higher temperatures we can see that the effect of temperature on the fluoride adsorption was small. The kinetic parameters obtained for Langmuir and Freundlich isotherm fittings are shown in Table 1. According to Table 1, the adsorption of fluoride by Ms-La was more consistent with Langmuir isotherm than that of the Freundlich isotherm. The maximum adsorption capacity was 19.85 mg/g with a correlation coefficient of 0.9968. The comparison of Q_m with some other adsorbents (Table 2) also suggests that the Ms-La should be a good medium for the treatment of fluoride contaminated water.

3.4.2. Adsorption mechanisms

It can be seen from the SEM images that the appearance of the adsorbent had changed greatly. A lot of powder fragments had appeared in the adsorbed material, which shows that the material has changed during the adsorption process and a new material has formed. The properties of the adsorbent were significantly changed as can be seen by the XRD analysis. The material was mainly lanthanum carbonate before adsorption, part of the carbonate was replaced by F^- to form a new material $La(CO_3)F$ during the adsorption process. Mechanism of fluoride removal by the Ms-La belongs to the typical ion exchange adsorption, which may be expressed as follows:

$$\text{Ms-La}_2(CO_3)_3 + 2F^- = \text{Ms-2LaCO}_3F + CO_3^{2-} \quad (4)$$

where Ms is a carrier of SiO_2.

4. Conclusion

In this study, mesoporous silica supporting lanthanum carbonate (Ms-La) with a good defluorination performance had been synthesized. The optimization experiments for synthesizing Ms-La samples have been conducted in this study and the optimal conditions were found to be: nNaHCO$_3$/nLa=3, nLa/nSi = 0.08, drying temperature = 90°C, the removal rate of fluoride ion was up to 90% when the materials were prepared via co-precipitation method. The Ms has a large specific surface area and rich channel, so it can improve the dispersion of rare earth compounds and increase the active points and effective contact area of Ms-La. Compared with pure $La_2(CO_3)_3$, Ms-La dispersed evenly which leads to its high utilization and capacity for the removal of F^-; there are little changes on XRD diffraction peak and the mesoporous structure. The adsorption process of Ms-La material followed Langmuir isotherm adsorption model, and the effect of temperature on adsorption was small, so it can be used to remove F^- from water at room temperatures. The maximum adsorption capacity was 19.85 mg/g with a correlation coefficient of 0.9968. The mechanism of $La_2(CO_3)_3$ defluorination is mainly based on the replacement of CO_3^{2-} by F^- to form $La(CO_3)F$.

Acknowledgements

This study was supported by YMU-DEAKIN International Associated Laboratory on Functional Materials, Key Laboratory of Resource Clean Conversion in Ethnic Region, Education Department of Yunnan Province (117-02001001002107). Scientific Research Fund Project, Education Department of Yunnan Province (2016YJS079).

References

[1] Z. Zhang, T. Yue, M. Zhong, Defluorination of wastewater by calcium chloride modified natural zeolite, Desalination, 276 (2011) 246–252.
[2] L. Chmielarz, P. Kuśtrowski, M. Kruszec, R. Dziembaj, P. Cool, E.F. Vansant, Nitrous oxide reduction with ammonia and methane over mesoporous silica materials modified with transition metal oxides, J. Porous Mater., 12 (2005) 123–129.
[3] M.M. Emamjomeh, M. Sivakumar, Fluoride removal by a continuous flow electrocoagulation reactor, J. Environ. Manage., 90 (2009) 1204–1212.

[4] D. Ghosh, C.R. Medhi, M.K. Purkait, Treatment of fluoride containing drinking water by electrocoagulation using monopolar and bipolar electrode connections, Chemosphere, 73 (2008) 1393–1400.
[5] L. Zhang, Y. Gao, M. Li, Expanded graphite loaded with lanthanum oxide used as a novel adsorbent for phosphate removal from water: performance and mechanism study, J. Environ. Technol., 36 (1900) 1016–1025.
[6] F. Luo, K.N. Ghimire, M. Kuriyama, Removal of fluoride using some lanthanum(III)-loaded adsorbents with different functional groups and polymer matrices, Chem. Technol. Biotechnol., 78 (2003) 1038–1047.
[7] J.J. Sun, L.J. Xu, New progress in modification and application of nanosilicon dioxide, J. Phys. Chem., 4 (2012) 52–58 (in Chinese).
[8] X. Ding, X.C. Yu, H.X. Sun, Preparation and characterization of MCM-41 mesoporous silica functionalized with sulfonic acid groups, Adv. Mater. Res., 781–784 (2013) 215–218.
[9] S. Jagtap, M.K. Yenkie, S. Das, Synthesis and characterization of lanthanum impregnated chitosan flakes for fluoride removal in water, Desalination, 273 (2011) 267–275.
[10] K.J. Ewing, L. Buckner, J. Jaganathan, Preparation of high purity lanthanum compounds for use in fluoride optical fibers, Mater. Res. Bull., 24 (1989) 163–168.
[11] T. Wei, G.Z. Li, T.L. Wang, M. Yang, J.H. Peng, C.J. Barrow, W.R. Yang, H.B. Wang, Preparation and adsorption of phosphorus by new heteropolyacid salt-lanthanum oxide composites, Desal. Wat. Treat., 57 (2016) 7874–7880.
[12] W. Wang, The removal of fluoride ion from aqueous solution by a cation synthetic resin, Sep. Sci. Technol., 37 (2002) 89–103.
[13] M.S. Onyango, Y. Kojima, O. Aoyi, Adsorption equilibrium modeling and solution chemistry dependence of fluoride removal from water by trivalent-cation-exchange zeolite, J. Colloid Interface Sci., 279 (2004) 341–350.
[14] R.R. Li, Y. Shi, L. Zu, H.Q. Lian, Y. Liu, X.G. Cui, The preparation and characterization of the mesoporous poly(bisphenol-A carbonate) – silicananocomposites, Appl. Mech. Mater., 513–517 (2014) 82–85.
[15] L.J. Zhang, X. Hu, C.Z. Yu, R. Crawford, A. Yu, Preparation of sinapinaldehyde modified mesoporous silica materials and their application in selective extraction of trace Pb(II), Int. J. Environ. Anal. Chem., 93 (2013) 1274–1285.
[16] F. Agnes, K. Yoshimichi, M. Fujio, T. Makoto, I. Shu-IchiNiwa, Preparation of mesoporous composite materials by pillaring of magadiite with silica, Mol. Crystals Liq. Crystals Sci. Technol. Sect. A: Mol. Crytals Liq. Crystals, 311 (1998) 321–326.
[17] B. Naik, N.N. Ghosh, A review on chemical methodologies for preparation of mesoporous silica and alumina based materials, Recent Pat. Nanotechnol., 3 (2009) 213–217.
[18] Z. Wang, D.M. Fang, Q. Li, Z.L. Xia, R.Q,Y. Zhu, H.Y. Qu, Y.P. Du, Modified mesoporous silica materials for on-line separation and preconcentration of hexavalent chromium using a microcolumn coupled with flame atomic absorption spectrometry, Anal. Chim. Acta, 725 (2012) 81–86.
[19] L.M. Shan, Z.H. Li, W.Z. Z, Removal of F^- in zinc oxide dust purification solution by cerium salt method, Hydrometallurgy China, 33 (2014) 142–144 (in Chinese).
[20] G.P. Ma, Z.R. Liu, C.L. Zhao, Study on adsorption and removal of fluoride from lanthanum oxidation film silica gel, Chin. J. Environ. Sci., 19 (1999) 58–61 (in Chinese).
[21] S. Liu, R.J. Ma, Infrared spectra of rare earth carbonate, Sci. Technol. Eng., 7 (2007) 1430–1433 (in Chinese).
[22] E. Kumar, A. Bhatnagar, M. Ji, Defluoridation from aqueous solutions by granular ferric hydroxide (GFH), Water Res., 43 (2009) 490–498.
[23] L. Chen, Granulation of Fe-Al-Ce nano-adsorbent for fluoride removal from drinking water by spray coating on sand in a fluidized bed, Powder Technol., 193 (2009) 59–64.
[24] M. Karthikeyan, K.P. Elango, Removal of fluoride from water using aluminium containing compounds, Environ. Sci., 21 (2009) 1513–1518.
[25] K.B. Li, X.L. Tang, L. Guo, T. Zhang, Study on adsorption performance for fluoride by chitosan supported lanthanum, J. Hunan Univ. Sci. Technol., 24 (2009) 113–117 (in Chinese).
[26] E. Kusrini, N. Sofyan, N. Suwartha, Chitosan-praseodymium complex for adsorption of fluoride ions from water, J. Rare Earths, 33 (2015) 1104–1113.
[27] M. Ravanipour, R. Kafaei, M. Keshtkar, Fluoride ion adsorption onto palm stone: optimization through response surface methodology, isotherm, and adsorbent characteristics data, Data in Brief, 12 (2017) 471–479.